Computer Assisted Mechanics and Engineering Sciences, **3**: 263–282, 1996.


# Parameter sensitivity of metal forming processes

Horacio Javier Antunez and Michał Kleiber
*Institute of Fundamental Technological Research, Polish Academy of Sciences*
*00-049 Warszawa, ul. Świętokrzyska 21*

(Received August 23, 1996)

The flow formulation for metal forming analysis based on a rigid-viscoplastic material model is considered. Specifically, sensitivity evaluation techniques are discussed for different solution variables with respect to variations in parameters entering the constitutive (and other) equations such as material constants, imposed velocities or friction coefficient. A method to avoid spurious pressure modes is introduced which allows to use Q1/Q1 elements and thus to accurately calculate pressures, their sensitivities and friction forces. In addition, one pressure unknown for each node is available in this method, thus yielding a finer discretisation for this variable.

## 1. Introduction

One of the first approaches to analyse metal forming processes was the so-called flow formulation, initiated by Goon *et al.* [1], which has since then attracted the attention of researchers for its simplicity and versatility. A complete presentation of the approach was given by Zienkiewicz *et al.* [2]. Situations frequently met in metal forming processes are well accounted for by considering the metal as a non-Newtonian fluid, neglecting the elastic strains during the processes (since they are much smaller than the plastic ones), and, if needed, calculating them additionally at the end of the analysis. The method is best suited for stationary processes in which the Eulerian approach considerably simplifies the analysis. The primary variables are the velocities $v_i$ of the deforming body. A rigid-viscoplastic model thus results as a means to describe the material behaviour with a set of equations analogous to that of a non-Newtonian fluid; the use of the flow approach is therefore justified. For transient cases different approaches have been proposed that take into account changes in the configuration due to the movement of the tools, progress of the free surfaces, contact zone developments, etc. Because of the low velocities which normally take place in these processes accurate results are obtained by first solving the problem for a fixed configuration, and then updating it for the incremented time.

The adequacy of such an approach has been both supported and criticised, and it is not our objective here to comment on that aspect. Our pragmatic viewpoint is, however, that the method is well suited for solving many problems frequently encountered in metal forming practice.

The sensitivity analysis was first developed for 2D stress problems by Zienkiewicz and Campbell [3]. Other applications in structural analysis followed by using both the so called direct differentiation method (DDM) and the adjoint system method (ASM) as discussed by Haug [4], Haug and Arora [5], Haug *et al.* [6], Ryu *et al.* [7], Yang and Botkin [8], Raju *et al.* [9], Kleiber *et al.* [10], among others. Useful information regarding the influence of material properties, geometric parameters, etc. on the results is available from such an analysis at a numerical cost which is small compared to the solution of the equilibrium analysis problem. At the same time the sensitivity analysis may constitute a crucial step in optimisation of the process on hand. On the basis of the sensitivity information a set of optimum design conditions can be satisfied; one can aim at minimising the plastic deformation energy, the distortion suffered by the material, the maximum temperature reached, etc.

In this paper the sensitivity analysis of metal forming processes with respect to parameters entering the material model is presented. The flow formulation is adopted for the analysis of the mechanical problem. Both the ASM and DDM are discussed. It is shown that the tangent matrix used in the analysis problem can most frequently be also used for solving the sensitivity problem, yielding a linear system of equations with the same governing matrix but a different right-hand side vector as the only additional quantity to be computed at the sensitivity stage. Finally, the iterative (secant stiffness matrix based) version of both the ASM and DDM is developed and applied to the solution of a particular problem where the tangent stiffness matrix cannot be used on grounds of its ill-conditioning.

## 2. Flow approach for metal forming analysis

We shall briefly present in this section the set of equations typical of the flow formulation. Using notation which has already been standardised in the literature [2], continuum equations describing the rigid-viscoplastic flow are as follows:

$$\begin{aligned} \sigma_{ij} &= s_{ij} - p\,\delta_{ij}\,, \\ s_{ij} &= 2\mu\,\dot{\varepsilon}_{ij}\,, \\ \dot{\varepsilon}_{ij} &= \tfrac{1}{2}(v_{i,j} + v_{j,i})\,, \\ \dot{\varepsilon}_{kk} &= 0\,, \\ \mu &= \frac{\sigma_0 + (\dot{\bar{\varepsilon}}/\gamma)^{\frac{1}{n}}}{3\dot{\bar{\varepsilon}}}\,, \qquad \dot{\bar{\varepsilon}} = \sqrt{\tfrac{2}{3}\dot{\varepsilon}_{ij}\dot{\varepsilon}_{ij}}\,, \end{aligned} \tag{1}$$

where $\mu$ is the nonlinear viscosity, $\sigma_0$ the static tensile yield limit, $s_{ij}$ the stress deviator, $p$ the pressure (assumed positive in compression) and $\gamma, n$ parameters of the model. The weak form of the equilibrium equation reads

$$\int_\Omega \boldsymbol{\sigma}\cdot\dot{\boldsymbol{\varepsilon}}\;\mathrm{d}\Omega = \int_\Omega \hat{\mathbf{f}}\,\mathbf{v}\;\mathrm{d}\Omega + \int_{\partial\Omega_t} \hat{\mathbf{t}}\,\mathbf{v}\;\mathrm{d}\,(\partial\Omega) \tag{2}$$

We now introduce the mixed FEM expansion (the standard matrix notation is used)

$$\begin{aligned} v_i &= \mathbf{N}\dot{\mathbf{q}}_i, \quad i = 1,2,\ldots,I\,, \\ \dot{\boldsymbol{\varepsilon}} &= \mathbf{B}\dot{\mathbf{q}}\,, \\ p &= \bar{\mathbf{B}}\bar{\mathbf{p}}\,, \end{aligned} \tag{3}$$

where $\mathbf{N}$ and $\bar{\mathbf{B}}$ are the shape functions for the velocity and pressure and $\mathbf{B}$ is the standard strain rate-velocity matrix while $\dot{\mathbf{q}} = \{\dot{q}_\alpha\} = \{\dot{\mathbf{q}}_1^1, \ldots, \dot{\mathbf{q}}_I^1, \dot{\mathbf{q}}_1^2, \ldots, \dot{\mathbf{q}}_I^2, \ldots, \dot{\mathbf{q}}_1^{\hat{N}}, \ldots, \dot{\mathbf{q}}_I^{\hat{N}}, \}$, $\alpha = 1,2,\ldots,N$ and $\bar{\mathbf{p}} = \{\bar{p}_{\bar{\alpha}}\}$, $\bar{\alpha} = 1,2,\ldots,\bar{N}$ are the nodal velocity and pressure vectors, respectively, with $N$ and $\bar{N}$ denoting the respective numbers of kinematic and pressure degrees of freedom, $I$ the number of velocity components (i.e. $I = 2$ or $I = 3$) and $\hat{N}$ the number of nodes for velocity discretisation (hence $N = I\cdot\hat{N}$). The vector $\dot{\mathbf{q}}$ is split in $I$ vectors $\dot{\mathbf{q}}_i$ each consisting of subsequent nodal velocity components along the '$i$'-axis. By splitting $\mathbf{Q}$, $\hat{\mathbf{f}}$ and $\hat{\mathbf{t}}$ in the same way as $\dot{\mathbf{q}}$, we obtain from Eq. (2)

$$\int_\Omega \mathbf{B}^{\mathrm{T}}\boldsymbol{\sigma}\;\mathrm{d}\Omega = \mathbf{Q}\,, \tag{4}$$

$$\mathbf{Q}_i = \int_\Omega \mathbf{N}\hat{\mathbf{f}}_i\;\mathrm{d}\Omega + \int_{\partial\Omega_t} \mathbf{N}\hat{\mathbf{t}}_i\;\mathrm{d}\,(\partial\Omega) + \mathbf{F}_i\,, \tag{5}$$

in which the superscript 'T' indicates transposition and $\mathbf{F}$ is the vector of concentrated loads applied at the nodes. By substituting Eq. (1) into it we get

$$\left(\int_{\Omega} 2\mu\, \mathbf{B}^{\mathrm{T}}\mathbf{B}\; \mathrm{d}\Omega\right)\dot{\mathbf{q}} - \left(\int_{\Omega} \mathbf{B}^{\mathrm{T}}\mathbf{m}\,\bar{\mathbf{B}}\; \mathrm{d}\Omega\right)\bar{\mathbf{p}} = \mathbf{Q}\,, \tag{6}$$

i.e.

$$\mathbf{K}_{(\mu)}\dot{\mathbf{q}} + \mathbf{K}_{(p)}^{\mathrm{T}}\bar{\mathbf{p}} = \mathbf{Q} \tag{7}$$

with

$$\begin{aligned} \mathbf{K}_{(\mu)} &= \int_{\Omega} \mu\, \mathbf{k}_0\; \mathrm{d}\Omega = \int_{\Omega} 2\mu\, \mathbf{B}^{\mathrm{T}}\mathbf{B}\; \mathrm{d}\Omega\,, \\ \mathbf{K}_{(p)}^{\mathrm{T}} &= -\int_{\Omega} \mathbf{B}^{\mathrm{T}}\mathbf{m}\,\bar{\mathbf{B}}\; \mathrm{d}\Omega\,, \end{aligned} \tag{8}$$

the row vector $\mathbf{m} = [1\ 1\ 1\ 0\ 0\ 0]$ converting the total strain into the volumetric component and $\mathbf{k}_0$ being dependent only on the geometry.

The equilibrium equation (2) has to be solved together with the incompressibility condition $(1)_4$ written in the weak form as

$$\int_{\Omega} \bar{\mathbf{B}}\dot{\varepsilon}_{kk}\; \mathrm{d}\Omega = \mathbf{0}\,, \tag{9}$$

which after discretisation reads

$$\left(\int_{\Omega} \bar{\mathbf{B}}^{\mathrm{T}}\,\mathbf{m}^{\mathrm{T}}\mathbf{B}\; \mathrm{d}\Omega\right)\dot{\mathbf{q}} = 0 \tag{10}$$

or, more compactly

$$\mathbf{K}_{(p)}\dot{\mathbf{q}} = 0\,. \tag{11}$$

The fundamental set of equations becomes

$$\begin{bmatrix} \mathbf{K}_{(\mu)} & \mathbf{K}_{(p)}^{\mathrm{T}} \\ \mathbf{K}_{(p)} & \mathbf{0} \end{bmatrix} \begin{bmatrix} \dot{\mathbf{q}} \\ \bar{\mathbf{p}} \end{bmatrix} = \begin{bmatrix} \mathbf{Q} \\ \mathbf{0} \end{bmatrix} \tag{12}$$

or, shorter, in the residual form

$$\mathbf{R} = \bar{\mathbf{K}}_{(\mu)}\bar{\mathbf{q}} - \bar{\mathbf{Q}} = \mathbf{0}\,. \tag{13}$$

Equation (12) corresponds to the equations describing the nonlinear Stokes flow. The dynamic terms are not included, which is justified by the fact that usually low velocities prevail in metal forming processes. For a typical metal forming case (like extrusion) the Reynolds number is of the order of $10^{-9}$.

The matrix $\bar{\mathbf{K}}_{(\mu)}$ depends on the solution through the solution dependent viscosity $\mu$ so that an iterative process is generally needed to find the solution vector $\bar{\mathbf{q}}$. At the $i$-th iteration Eq. (13) reads

$$\mathbf{R}^{(i)} = \bar{\mathbf{K}}_{(\mu)}^{(i)}\bar{\mathbf{q}}^{(i)} - \bar{\mathbf{Q}}\,. \tag{14}$$

In order to employ the Newton–Raphson method we write the next iteration residual approximated by the first order Taylor expansion

$$\mathbf{R}^{(i+1)} \cong \mathbf{R}^{(i)} + \frac{\partial \mathbf{R}^{(i)}}{\partial \bar{\mathbf{q}}}\delta\bar{\mathbf{q}}^{(i+1)} = 0 \tag{15}$$

from which the solution correction is computed as

$$\delta\bar{\mathbf{q}}^{(i+1)} = -\left(\frac{\partial \mathbf{R}^{(i)}}{\partial \bar{\mathbf{q}}}\right)^{-1} \mathbf{R}^{(i)}, \qquad \bar{\mathbf{q}}^{(i+1)} = \bar{\mathbf{q}}^{(i)} + \delta\bar{\mathbf{q}}^{(i+1)}, \tag{16}$$

where

$$\frac{\partial \mathbf{R}^{(i)}}{\partial \bar{\mathbf{q}}} = \bar{\mathbf{K}}_{(\mu)} + \int_\Omega (\bar{\mathbf{k}}_0 \bar{\mathbf{q}}) \frac{\partial \mu}{\partial \bar{\mathbf{q}}} \, d\Omega = \mathbf{K}^t_{(\mu)}, \qquad \bar{\mathbf{k}}_0 = \begin{bmatrix} \mathbf{k}_0 & \mathbf{0} \\ \mathbf{0} & \mathbf{0} \end{bmatrix} \tag{17}$$

is the (non–symmetric) tangent stiffness matrix while

$$\frac{\partial \mu}{\partial \dot{q}_\alpha} = \frac{\partial \mu}{\partial \bar{\varepsilon}} \frac{\partial \dot{\bar{\varepsilon}}}{\partial \dot{\varepsilon}_{ij}} \frac{\partial \dot{\varepsilon}_{ij}}{\partial \dot{q}_\alpha} = -\left[\sigma_0 + \left(1 - \frac{1}{n}\right)\left(\frac{\dot{\bar{\varepsilon}}}{\gamma\sqrt{3}}\right)^{\frac{1}{n}}\right] \frac{2\dot{\varepsilon}_{ij}}{\sqrt{3}\dot{\bar{\varepsilon}}^3} B_{ij\alpha}, \tag{18}$$

$$\frac{\partial \mu}{\partial \bar{p}} = 0. \tag{19}$$

Since stationary problems are considered only, no time integration is needed; otherwise, for an implicit scheme the computation of the contribution of the load term $\mathrm{d}\mathbf{Q}/\mathrm{d}\bar{\mathbf{q}}$ to the tangent stiffness matrix would be required.

The formulation of the boundary value problem is completed by a suitable specification of the boundary conditions, which can be either of sticking or no-friction sliping-type, or of an intermediate type defined by a tangential force applied to the material boundary and computed according to a given friction law. A simple way of modelling this last option, as suggested by Zienkiewicz [2], is to insert a thin layer of elements connecting the fixed boundary with the material. According to the Coulomb friction law, a yield stress proportional to pressure is assigned to the elements so that the material is acted upon by a tangential force proportional to the force normal to the boundary and directed opposite to the material movement. If the pressure happens to be zero, a residual viscosity is imposed in order to avoid numerical singularity of the matrices.

The application of such an algorithm requires an accurate enough pressure evaluation. It is a known fact that for nonlinear problems the so-called Babuska–Brezzi condition is not satisfied even by the Q2/Q1 elements and spurious pressure modes appear. Hughes *et al.* [11] have proposed a method for pressure stabilisation circumventing the Babuska–Brezzi condition, in which the equilibrium equation, suitably weighted by the gradient of the shape functions, is added to the pressure equation in order to obtain the negative Laplacian in the diagonal block for the pressure, which is responsible for the stabilising effect. The added equation should vanish when the converged solution is reached. By applying this technique to the flow formulation for metal forming problems we add to the incompressibility condition (10) the equation

$$\int_\Omega \frac{\alpha h^2}{2\mu} (\nabla \bar{\mathbf{B}} \cdot (-\nabla \cdot \mathbf{s} + \nabla p - \mathbf{f})) \, d\Omega = 0, \tag{20}$$

where $\alpha$ is a stabilisation coefficient, $0 \leq \alpha \leq 1$, $h$ is a characteristic magnitude for each element (the mesh size), and $\mathbf{s}$ is, as before, the stress deviator. For $\alpha = 0$ the system of equations reduces to the standard formulation and the solution will not converge unless the Babuska–Brezzi condition is fulfilled.

The equations for the pressure assume the form

$$(\mathbf{K}_{(p)} + \mathbf{L})\dot{\mathbf{q}} + \mathbf{M}\mathbf{p} = \mathbf{H}, \tag{21}$$

where

$$
\begin{aligned}
\mathbf{L} &= [\mathbf{L}_1\,\mathbf{L}_2]\,,\\
\mathbf{L}_1 &= -\int_\Omega \frac{\alpha h^2 k_p}{2\mu}\left(\bar{\mathbf{B}}_{,1}\frac{\partial}{\partial x_1}(\mu(2\mathbf{N}^{\mathrm{T}}_{,1}+\mathbf{N}^{\mathrm{T}}_{,2}))+\bar{\mathbf{B}}_{,2}\frac{\partial}{\partial x_2}(\mu\mathbf{N}^{\mathrm{T}}_{,2})\right)\,\mathrm{d}\Omega\,,\\
\mathbf{L}_2 &= -\int_\Omega \frac{\alpha h^2 k_p}{2\mu}\left(\bar{\mathbf{B}}_{,1}\frac{\partial}{\partial x_1}(\mu\mathbf{N}^{\mathrm{T}}_{,1})+\bar{\mathbf{B}}_{,2}\frac{\partial}{\partial x_2}\left(\mu(\mathbf{N}^{\mathrm{T}}_{,1}+2\mathbf{N}^{\mathrm{T}}_{,2})\right)\right)\,\mathrm{d}\Omega\,,\\
\mathbf{M} &= \int_\Omega \frac{\alpha h^2 k_p^2}{2\mu}\bar{\mathbf{B}}_{,i}\bar{\mathbf{B}}^{\mathrm{T}}_{,i}\,\mathrm{d}\Omega\,,\\
\mathbf{H} &= \int_\Omega \frac{\alpha h^2 k_p^2}{2\mu}\bar{\mathbf{B}}_{,i}f_i\,\mathrm{d}\Omega
\end{aligned}
\tag{22}
$$

and $k_p$ is a scaling factor for the pressure [12]. The element matrices will in general be non-symmetric except for linear interpolations, in which case the second derivatives of the shape functions vanish. The submatrix $\mathbf{M}$ connecting pressures at different points is the negative discrete Laplacian which is responsible for the stabilising effect. In this paper the formulation has been implemented for Q1/Q1 shape functions (hence $\bar{\mathbf{B}} = \mathbf{N}$) within the finite element code for metal forming analysis developed by the first author [13].

Having discussed the way to remove the spurious pressure modes we may pass on to the treatment of friction. In the element layers where friction is considered to take place we assume that the viscosity is given by

$$\mu = \frac{\sigma_f}{3\dot{\bar{\varepsilon}}} \tag{23}$$

with $\sigma_f$ defined as

$$
\sigma_f = \begin{cases} \sigma_{vp} = \sigma_0 + (\dot{\bar{\varepsilon}}/\gamma)^{\frac{1}{n}}\,, & \text{if} \quad pf > \sigma_{vp}\,,\\ pf\,, & \text{if} \quad 0 < pf < \sigma_{vp}\,,\\ \delta\,, & \text{if} \quad p \le 0\,. \end{cases}
\tag{24}
$$

In this way the more compressed the material against the surface, the bigger the shear stress between the friction layer and the rest of the material.

For the friction elements the derivatives (18) and (19) take the form

$$
\frac{\partial \mu}{\partial \dot{q}_\alpha} = \begin{cases} -\frac{pf}{3\dot{\bar{\varepsilon}}^3}2\dot{\varepsilon}_{ij}B_{ij\alpha}\,, & \text{if} \quad 0 < pf < \sigma_{vp}\,,\\ -\frac{\delta}{3\dot{\bar{\varepsilon}}^3}2\dot{\varepsilon}_{ij}B_{ij\alpha}\,, & \text{if} \quad p \le 0\,, \end{cases}
\tag{25}
$$

and

$$\frac{\partial \mu}{\partial p} = \frac{f}{3\dot{\bar{\varepsilon}}}\,, \qquad \text{if} \quad 0 < pf < \sigma_{vp}\,. \tag{26}$$

### 3. Sensitivity analysis

We consider now a general form of the performance function as

$$\phi = \phi(\mathbf{s}, \bar{\mathbf{q}}; h). \tag{27}$$

We wish to calculate the sensitivity of $\phi$ with respect to a material parameter $h$ entering the theory. As $h$ we may take $n$, $\gamma$, or $\sigma_0$, *cf.* Eq. (1). Following the so-called direct differentiation method (DDM) we calculate the gradient

$$\frac{\mathrm{d}\phi}{\mathrm{d}h} = \frac{\partial\phi}{\partial h} + \frac{\partial\phi}{\partial\mathbf{s}}\frac{\mathrm{d}\mathbf{s}}{\mathrm{d}h} + \frac{\partial\phi}{\partial\bar{\mathbf{q}}}\frac{\mathrm{d}\bar{\mathbf{q}}}{\mathrm{d}h}, \tag{28}$$

in which, given the solution of the equilibrium problem, $\partial\phi/\partial h$, $\partial\phi/\partial\bar{\mathbf{q}}$ and $\partial\phi/\partial\mathbf{s}$ are known, or can be routinely obtained, and $\mathrm{d}\mathbf{s}/\mathrm{d}h$ can be written in an easily computable way as

$$\frac{\mathrm{d}\mathbf{s}}{\mathrm{d}h} = \frac{\mathrm{d}\mathbf{s}}{\mathrm{d}\bar{\mathbf{q}}}\frac{\mathrm{d}\bar{\mathbf{q}}}{\mathrm{d}h}, \tag{29}$$

where $\frac{\mathrm{d}\mathbf{s}}{\mathrm{d}\bar{\mathbf{q}}} = \left\{\frac{\mathrm{d}\mathbf{s}}{\mathrm{d}\dot{\mathbf{q}}}\,\frac{\mathrm{d}\mathbf{s}}{\mathrm{d}\bar{\mathbf{p}}}\right\}$, and, according to Eqs. (4), (6) and (1)

$$\begin{aligned}\frac{\mathrm{d}\mathbf{s}}{\mathrm{d}\dot{\mathbf{q}}} &= 2\mu\mathbf{B} + 2\frac{\partial\mu}{\partial\dot{\mathbf{q}}}\mathbf{B}\dot{\mathbf{q}},\\ \frac{\mathrm{d}\mathbf{s}}{\mathrm{d}\bar{\mathbf{p}}} &= \mathbf{0}.\end{aligned} \tag{30}$$

Therefore, in order to compute $\mathrm{d}\phi/\mathrm{d}h$ by Eq. (28) only $\mathrm{d}\mathbf{q}/\mathrm{d}h$ has to be obtained from additional calculations. By differentiating the equilibrium equation (13) with respect to $h$ we have

$$\frac{\mathrm{d}}{\mathrm{d}h}\left(\bar{\mathbf{K}}_{(\mu)}\bar{\mathbf{q}} - \bar{\mathbf{Q}}\right) = \frac{\mathrm{d}\bar{\mathbf{K}}_{(\mu)}}{\mathrm{d}h}\bar{\mathbf{q}} + \bar{\mathbf{K}}_{(\mu)}\frac{\mathrm{d}\bar{\mathbf{q}}}{\mathrm{d}h} - \frac{\mathrm{d}\bar{\mathbf{Q}}}{\mathrm{d}h} = \mathbf{0}, \tag{31}$$

where

$$\frac{\mathrm{d}\bar{\mathbf{K}}_{(\mu)}}{\mathrm{d}h} = \int_\Omega \frac{\partial\mu}{\partial h}\bar{\mathbf{k}}_0\,\mathrm{d}\Omega + \int_\Omega\left(\frac{\partial\mu}{\partial\bar{\mathbf{q}}}\frac{\mathrm{d}\bar{\mathbf{q}}}{\mathrm{d}h}\right)\bar{\mathbf{k}}_0\,\mathrm{d}\Omega. \tag{32}$$

By combining Eqs. (31) and (32) we arrive at

$$\left(\bar{\mathbf{K}}_{(\mu)} + \int_\Omega(\bar{\mathbf{k}}_0\bar{\mathbf{q}})\frac{\partial\mu}{\partial\bar{\mathbf{q}}}\,\mathrm{d}\Omega\right)\frac{\mathrm{d}\bar{\mathbf{q}}}{\mathrm{d}h} = -\left(\int_\Omega\frac{\partial\mu}{\partial h}\bar{\mathbf{k}}_0\,\mathrm{d}\Omega\right)\bar{\mathbf{q}}, \tag{33}$$

i.e., at

$$\mathbf{K}^t_{(\mu)}\frac{\mathrm{d}\bar{\mathbf{q}}}{\mathrm{d}h} = -\left(\int_\Omega\frac{\partial\mu}{\partial h}\bar{\mathbf{k}}_0\,\mathrm{d}\Omega\right)\bar{\mathbf{q}}. \tag{34}$$

This equation can be used for finding the nodal velocity and pressure design gradients $\mathrm{d}\bar{\mathbf{q}}/\mathrm{d}h$ provided the nodal velocity and pressure vector $\bar{\mathbf{q}}$ has been solved for from the equilibrium problem.

We can equivalently solve the sensitivity problem by the so-called adjoint system method (ASM), for which we construct an extended functional $\mathcal{L} = \mathcal{L}[\mathbf{s}, \bar{\mathbf{q}}; h; \boldsymbol{\lambda}]$ as

$$\mathcal{L} = \phi + \boldsymbol{\lambda}^{\mathrm{T}}\mathbf{R}, \tag{35}$$

in which the state equation $\mathbf{R} = 0$ is the same as before, *cf.* Eq. (13) and $\boldsymbol{\lambda}$ is a $(N+\bar{N})$-dimensional kinematically admissible adjoint vector such that $\mathcal{L}$ is stationary with respect to $\bar{\mathbf{q}}$, i.e.

$$\frac{\mathrm{d}\mathcal{L}}{\mathrm{d}\bar{\mathbf{q}}} = \mathbf{0}. \tag{36}$$

We have

$$\frac{\mathrm{d}\mathcal{L}}{\mathrm{d}h} = \frac{\mathrm{d}\phi}{\mathrm{d}h} + \frac{\mathrm{d}\boldsymbol{\lambda}^{\mathrm{T}}}{\mathrm{d}h}\mathbf{R} + \boldsymbol{\lambda}^{\mathrm{T}}\frac{\mathrm{d}\mathbf{R}}{\mathrm{d}h}, \tag{37}$$

which simplifies to

$$\frac{\mathrm{d}\mathcal{L}}{\mathrm{d}h} = \frac{\mathrm{d}\phi}{\mathrm{d}h}, \tag{38}$$

because the state equation holds true for both the current and modified value of $h$. Furthermore

$$\frac{\mathrm{d}\mathcal{L}}{\mathrm{d}h} = \frac{\partial\mathcal{L}}{\partial h} + \frac{\partial\mathcal{L}}{\partial\bar{\mathbf{q}}}\frac{\mathrm{d}\bar{\mathbf{q}}}{\mathrm{d}h}, \tag{39}$$

which by Eqs. (36) and (38) becomes

$$\frac{\mathrm{d}\phi}{\mathrm{d}h} = \frac{\partial\mathcal{L}}{\partial h} \tag{40}$$

and can be directly used for the computation of the sensitivity $\mathrm{d}\phi/\mathrm{d}h$ required. The vector $\boldsymbol{\lambda}$ is computed from Eq. (36) in a non-iterative way as

$$\frac{\mathrm{d}\mathcal{L}}{\mathrm{d}\bar{\mathbf{q}}} = \frac{\mathrm{d}\phi}{\mathrm{d}\bar{\mathbf{q}}} + \boldsymbol{\lambda}^{\mathrm{T}}\left(\frac{\partial\bar{\mathbf{K}}_{(\mu)}}{\partial\bar{\mathbf{q}}}\bar{\mathbf{q}} + \bar{\mathbf{K}}_{(\mu)}\right) = \frac{\mathrm{d}\phi}{\mathrm{d}\bar{\mathbf{q}}} + \boldsymbol{\lambda}^{\mathrm{T}}\mathbf{K}^{t}_{(\mu)} = \mathbf{0}\,, \tag{41}$$

i.e. as

$$\mathbf{K}^{t\mathrm{T}}_{(\mu)}\boldsymbol{\lambda} = -\left(\frac{\mathrm{d}\phi}{\mathrm{d}\bar{\mathbf{q}}}\right)^{\mathrm{T}}, \tag{42}$$

in which

$$\frac{\mathrm{d}(\ldots)}{\mathrm{d}\bar{\mathbf{q}}} = \frac{\partial(\ldots)}{\partial\mathbf{s}}\frac{\mathrm{d}\mathbf{s}}{\mathrm{d}\bar{\mathbf{q}}} + \frac{\partial(\ldots)}{\partial\bar{\mathbf{q}}} \tag{43}$$

and $\mathrm{d}\mathbf{s}/\mathrm{d}\bar{\mathbf{q}}$ is given by Eq. (30). Since the stiffness matrix $\bar{\mathbf{K}}_{(\mu)}$ is non-symmetric, the solution of the adjoint system is not as straightforward as it is usually the case in structural mechanics problems. Instead, we are forced to use the transpose of the inverted system matrix in order to get $\boldsymbol{\lambda}$.

Experiences with solving metal forming problems described by Eq. (13) show, [12, 13, 14] that the Newton–Raphson scheme, (Eq. (15)), is applicable (i.e. it converges) only for markedly rate-dependent materials, like steel in hot working conditions. This corresponds (*cf.* [14]) to the exponent value $n < 2$ in the model (1). Thus, for a material behaviour closer to perfect plasticity direct iterations based on

$$\bar{\mathbf{K}}_{(\mu)}\left(\bar{\mathbf{q}}^{(i-1)}\right)\bar{\mathbf{q}}^{(i)} = \bar{\mathbf{Q}} \tag{44}$$

must be performed. This scheme is always convergent, although only linearly. Procedures for accelerating convergence have been analysed in [12].

In the present context the question arises whether the actual tangent stiffness matrix $\mathbf{K}^{t}_{(\mu)}$ or the secant stiffness matrix $\bar{\mathbf{K}}_{(\mu)}$ should be used for calculating the sensitivity. In the latter case the iterative version of DDM takes the form (*cf.* Eq. (34))

$$\bar{\mathbf{K}}_{(\mu)}\left(\frac{\mathrm{d}\bar{\mathbf{q}}}{\mathrm{d}h}\right)^{(i)} = -\left(\int_{\Omega}\frac{\partial\mu}{\partial h}\bar{\mathbf{k}}_0\,\mathrm{d}\Omega\right)\bar{\mathbf{q}} - \int_{\Omega}(\bar{\mathbf{k}}_0\bar{\mathbf{q}})\,\frac{\mathrm{d}\mu}{\mathrm{d}\bar{\mathbf{q}}}\,\mathrm{d}\Omega\left(\frac{\mathrm{d}\bar{\mathbf{q}}}{\mathrm{d}h}\right)^{(i-1)}. \tag{45}$$

Similarly, for ASM we have the iterative form equivalent to Eq. (42) as

$$\bar{\mathbf{K}}^{\mathrm{T}}_{(\mu)}\boldsymbol{\lambda}^{(i)} = -\left(\frac{\mathrm{d}\phi}{\mathrm{d}\bar{\mathbf{q}}}\right)^{\mathrm{T}} - \bar{\mathbf{q}}^{\mathrm{T}}\left(\frac{\partial\bar{\mathbf{K}}_{(\mu)}}{\partial\bar{\mathbf{q}}}\right)^{\mathrm{T}}\boldsymbol{\lambda}^{(i-1)}. \tag{46}$$

To compare both versions of the solution algorithm (tangent *vs.* secant stiffness) for sensitivity analysis, we have to keep in mind that frequently, as has been stated above, the equilibrium problem is solved by using the secant stiffness matrix so that its inverse is available at the end of that stage. If the problem could be solved by using the tangent stiffness matrix, then the decision which method to use is straightforward. Unfortunately, the Newton–Raphson method (which involves the use of the tangent stiffness matrix) is practically always divergent in the situations of most practical importance regarding sensitivity analysis, namely when no nonzero velocities are prescribed. From a practical point of view it is therefore important to critically evaluate both versions of the solution algorithm.

The tangent stiffness option with the well conditioned matrix yields the sensitivity solution in one step. On the other hand, whenever the equilibrium problem cannot be solved by the use of the tangent stiffness matrix, the solution to the new set of equations is required. In contrast, the secant stiffness option requires iterations but no new solution of the equations system. Moreover, when the material behaviour is close to ideal plasticity, the numerical inverse of the $\mathbf{K}^t_{(\mu)}$ matrix does not yield the solution in one step: it may be then necessary to iterate even with the tangent stiffness matrix just to improve the numerically unreliable one-pass solution. And it can happen that this iterative procedure is divergent, therefore the solution by the secant stiffness matrix as given by Eqs. (45) and (46) is compulsory. The question of superiority of one approach over the other is thus strongly dependent on the material behaviour, the way the loads are applied and the boundary conditions. This is further illustrated in Sec. **5**. In particular, for the perfectly plastic material the tangent matrix is singular and the solution variables become infinitely sensitive to changes in the physical properties if only the loads are held constant.

The equivalence of DDM and ASM can be shown by considering the case $\phi = q_\alpha$ ($\alpha$ being a specified component number), i.e. when the performance function coincides with a given nodal velocity. By Eq. (28) we have for DDM

$$\frac{\mathrm{d}q_\alpha}{\mathrm{d}h} = \mathbf{i}_{(\alpha)}\frac{\mathrm{d}\bar{\mathbf{q}}}{\mathrm{d}h} = -\mathbf{i}_{(\alpha)}\mathbf{K}^{t-1}_{(\mu)}\left(\int_\Omega \frac{\partial\mu}{\partial h}\bar{\mathbf{k}}_0\,\mathrm{d}\Omega\right)\bar{\mathbf{q}}\,, \tag{47}$$

where the $k$-th component of the vector $\mathbf{i}_{(\alpha)}(k)$ is $i^k_{(\alpha)} = \delta^k_\alpha$. For ASM, Eqs. (40) and (42) take the form

$$\frac{\mathrm{d}q_\alpha}{\mathrm{d}h} = \boldsymbol{\lambda}^{\mathrm{T}}_{(\alpha)}\frac{\partial\mathbf{R}}{\partial h} = \boldsymbol{\lambda}^{\mathrm{T}}_{(\alpha)}\left(\int_\Omega \frac{\partial\mu}{\partial h}\bar{\mathbf{k}}_0\,\mathrm{d}\Omega\right)\bar{\mathbf{q}} \tag{48}$$

and

$$\left(\mathbf{K}^t_{(\mu)}\right)^{\mathrm{T}}\boldsymbol{\lambda}_{(\alpha)} = -\mathbf{i}_{(\alpha)}\,, \tag{49}$$

where $\boldsymbol{\lambda}_{(\alpha)}$ is the adjoint vector corresponding to $\phi = q_{(\alpha)}$. Finally, substituting $\boldsymbol{\lambda}_{(\alpha)}$ from Eq. (49) into (48) we obtain Eq. (47). Moreover, taking the set of sensitivity functionals as $\boldsymbol{\phi} = \{\phi_\alpha\} = \{q_\alpha\} = \bar{\mathbf{q}}$, Eq. (42) takes the form

$$\left(\mathbf{K}^t_{(\mu)}\right)^{\mathrm{T}}\boldsymbol{\Lambda} = -\mathbf{I}\,, \tag{50}$$

where the $k$-th column of matrix $\boldsymbol{\Lambda}$ is the adjoint vector $\boldsymbol{\lambda}_{(\alpha)}$ for $\alpha = k$. From Eq. (40) we substitute $\boldsymbol{\Lambda}^{\mathrm{T}}$ in the expression for the sensitivities obtained by replacing in Eq. (40) $\phi$ by $\bar{\mathbf{q}}$, $\boldsymbol{\lambda}$ by $\boldsymbol{\Lambda}$ and $\mathcal{L}$ as given by Eq. (35), to get

$$\frac{\mathrm{d}\bar{\mathbf{q}}}{\mathrm{d}h} = \boldsymbol{\Lambda}^{\mathrm{T}}\frac{\partial\mathbf{R}}{\partial h} = -\mathbf{K}^{t}_{(\mu)}{}^{-1}\int_\Omega\left(\frac{\partial\mu}{\partial h}\bar{\mathbf{k}}_0\right)\bar{\mathbf{q}}\,\mathrm{d}\Omega\,, \tag{51}$$

which is equivalent to Eq. (34).

Usually, forming processes are conceived of by controlling (normally by holding constant) either the imposed velocity or the applied force. In the numerical model, as a result of the elimination of rows and columns corresponding to the fixed degrees of freedom during the solution procedure, the first case is equivalent to the application of external forces which are proportional to the viscosity, and through this dependence these applied forces are also a function of the design parameters. It comes out from the sensitivity analysis for the case of constant imposed velocities that the velocity field is all but insensitive to the material parameters, and only the pressure is sensitive to them. On the other hand, when fixed loads are imposed, the velocity exhibits a strong dependence on the value of the design parameters, while the pressure is almost constant. For this reason, this second case is discussed in the applications.

If we want to calculate the sensitivity of the solution to the material parameters entering the viscoplastic law we have to find, by Eq. (34), the partial derivative of the viscosity with respect to the given parameter. Equation (1) suggests the static yield stress $\sigma_0$, the fluidity $\gamma$ and the exponent $n$ of the viscoplastic law as possible parameters with respect to which we can analyse the sensitivity of the solution. We have in turn

$$\frac{\partial \mu}{\partial \sigma_0} = \frac{1}{\sqrt{3}\dot{\bar{\varepsilon}}}, \tag{52}$$

$$\frac{\partial \mu}{\partial \gamma} = -\frac{1}{\gamma n \sqrt{3}\dot{\bar{\varepsilon}}} \left( \frac{\dot{\bar{\varepsilon}}}{\gamma \sqrt{3}} \right)^{\frac{1}{n}}, \tag{53}$$

$$\frac{\partial \mu}{\partial n} = -\frac{1}{n^2 \sqrt{3}\dot{\bar{\varepsilon}}} \left( \frac{\dot{\bar{\varepsilon}}}{\gamma \sqrt{3}} \right)^{\frac{1}{n}} \ln \left( \frac{\dot{\bar{\varepsilon}}}{\gamma \sqrt{3}} \right). \tag{54}$$

We can also find the sensitivity to the friction coefficient by differentiating Eq. (23). This derivative will be non-zero only for some of the friction elements (those which are referred to in the second row of Eq. (24)), and it has the form

$$\frac{\partial \mu}{\partial f} = \frac{p}{\sqrt{3}\dot{\bar{\varepsilon}}}. \tag{55}$$

A further possibility, which may have potentially a great practical significance is to find the sensitivity to the imposed velocity. This means, for example, the sensitivity to the ram or forging hammer velocity, or to the tangential velocity of the roll, for extrusion, forge and rolling operations, respectively. In this case only the loads depend on the design parameter through the viscosity. Thus, if the tool effect is modeled by imposing a value proportional to $v_0$ to a subset $A = \left\{\hat{1}, \hat{2}, \ldots, \hat{\alpha}, \ldots\right\}$ of degrees of freedom, where $v_0$ is the tool velocity,

$$q_{\hat{\alpha}} = a_{\hat{\alpha}} v_0, \tag{56}$$

we define the vector $\boldsymbol{\gamma}$ such that

$$\gamma_\alpha = \begin{cases} \dfrac{q_\alpha}{v_0}, & \text{if} \quad \alpha \in A, \\ 0, & \text{else.} \end{cases} \tag{57}$$

We have $\gamma_\alpha = 0$ if either no value is imposed at the $\alpha$-th degree of freedom, or it is set to zero, or a velocity is imposed independently of $v_0$. In such a case, by recalling the sensitivity functional Eq. (27) we have

$$\frac{\mathrm{d}\phi}{\mathrm{d}v_0} = \frac{\mathrm{d}\phi}{\mathrm{d}q_\alpha}\gamma_\alpha = \frac{\mathrm{d}\phi}{\mathrm{d}\bar{\mathbf{q}}}\boldsymbol{\gamma}, \tag{58}$$

where $\dfrac{\mathrm{d}\phi}{\mathrm{d}q_\alpha}$ is the sensitivity of $\phi$ to the velocity $q_\alpha$, (i.e. $q_\alpha$ is taken as the design parameter).

## 4. Material model at low effective strain rates

Let us now go back for a moment to the material model. It is a known fact that the flow approach leads to numerical problems when the velocity field tends to be uniform rendering $\dot{\bar{\varepsilon}} \to 0$ with the viscosity $\mu$ tending to infinity (see the constitutive equation (1)). The traditional way of solving this problem (*cf.* [2]) is to define a cutoff value for the effective strain rate so that $\mu = \mu_{\text{lim}}$ for every $\dot{\bar{\varepsilon}} < \dot{\bar{\varepsilon}}_{\text{lim}}$. In addition, by pressure scaling a uniform order of magnitude can be obtained for the stiffness matrix elements, thus allowing a very small value for the effective strain rate limit. Nevertheless in some parts of the domain an "approximate" value of the viscosity will always be obtained. For the mechanical solution this is quite acceptable since the strain rate-viscosity curve is continuous. However, if we consider the tangent stiffness matrix (which is the system matrix for the sensitivity problem shown in Eqs. (34) and (42)), we notice that the elements of the partial derivative $\partial \bar{\mathbf{K}}_{(\mu)}/\partial \mathbf{q}$ are proportional to $\dot{\bar{\varepsilon}}^{-3}$ in the visco-plastic range, but are null in the "rigid flow" limit when a constant cutoff value is adopted –as described– for $\dot{\bar{\varepsilon}} < \dot{\bar{\varepsilon}}_{\text{lim}}$. This means that if the cutoff value for the effective strain rate is, say, $10^{-6}$, then there is a discontinuity of the order of O(18) in the effective strain rate limit. This jump clearly affects convergence of the Newton–Raphson scheme, and the agreement between the sensitivities as calculated by one of the "analytical" methods and by finite differences. This difficulty can be overcome in a simple way by replacing $\mu = \mu_{\text{lim}}$ in the interval $0 \le \dot{\bar{\varepsilon}} \le \dot{\bar{\varepsilon}}_{\text{lim}}$ by

$$\mu = \left. \frac{\mathrm{d}\mu}{\mathrm{d}\dot{\bar{\varepsilon}}} \right|_{\dot{\bar{\varepsilon}}=\dot{\bar{\varepsilon}}_{\text{lim}}} (\dot{\bar{\varepsilon}} - \dot{\bar{\varepsilon}}_{\text{lim}}) - \mu_{\text{lim}}\,, \tag{59}$$

that is, requiring a constant first derivative in the interval mentioned.

## 5. Numerical examples

### 5.1. Direct extrusion

As the first computational illustration of the forming process sensitivity analysis an extrusion matrix is considered as shown in Figure 1, with the given load applied at the left boundary representing the ram. The sticking friction conditions are assumed. The material model described by Eq. 1 is adopted

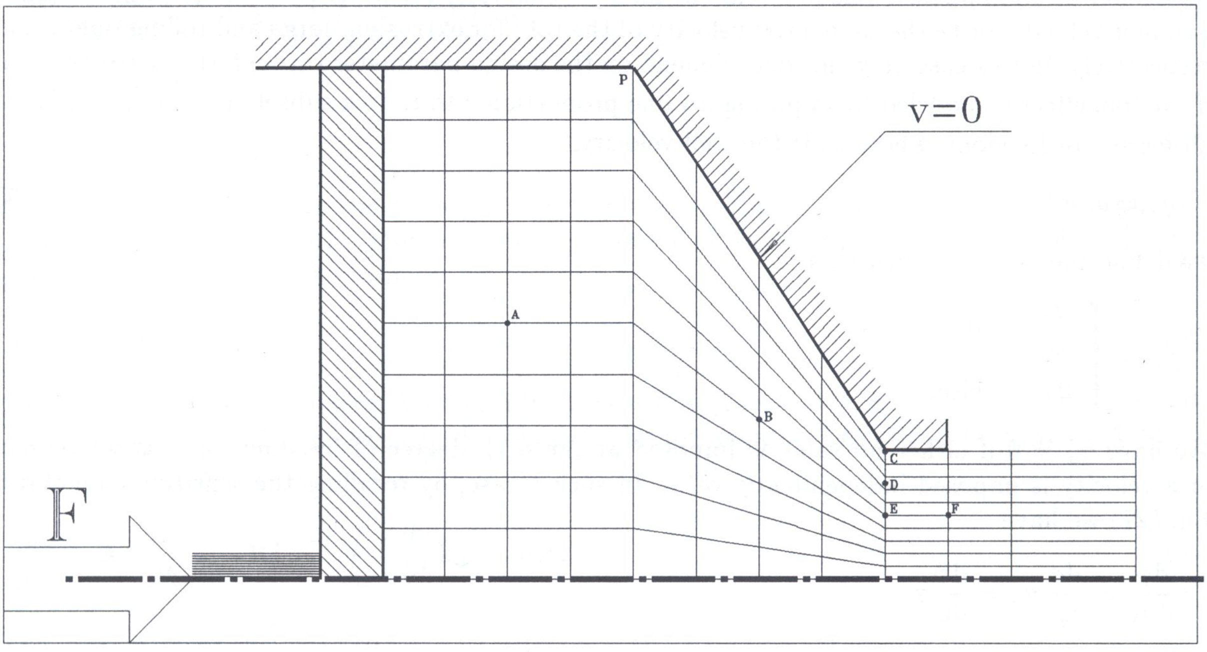


**Fig. 1.** Layout of the extrusion process and mesh 2

with $\sigma_0 = 200$, $\gamma = 0.1$ and $n = 1.5$. Free surface conditions prevail when the material gets out of the extrusion die. Sensitivity of the nodal variables $\mathbf{v}$ and $p$ with respect to the static yield stress $\sigma_0$ is calculated. Sensitivity isocurves of the velocity module are plotted in Figure 2. The character of the graph is very much similar to that for the isocurves of the velocity module. Both DDM and ASM have been employed. Both give the same results, which are also in full agreement with the finite difference method (FDM): no noticeable differences appear in the graphs. The case of the extrusion force held constant is considered next. In Figures 3 and 4 the velocity and pressure solution and their respective sensitivity at the points indicated as a function of the static yield stress are displayed. In each case the results for two different meshes are shown: the mesh No. 2 defined in Figure 1 and the mesh No. 1 such that every element of it contains four elements of the mesh No. 2.

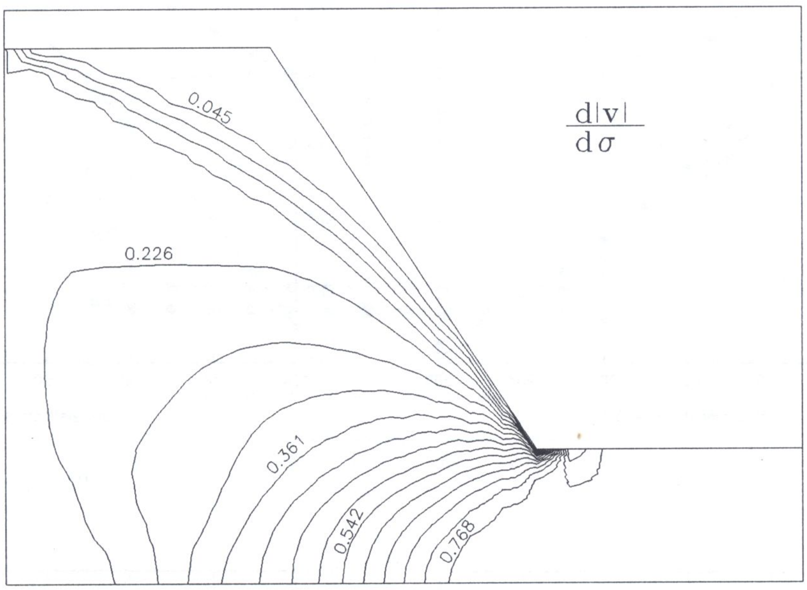


**Fig. 2.** Sensitivity of the velocity module to the static yield stress, $d||\mathbf{v}||/d\sigma_0$

In both cases the results are in very good agreement with the sensitivities calculated by FDM with the perturbations taken as $\Delta\sigma_0 = 1$. The plots are practically identical for any of the methods employed and the same mesh. As expected, velocities are more sensitive to changes in the static yield stress as the cross-section becomes smaller. Also, for constant loads the sensitivity of the velocity component in the direction at which the tool acts is negative since an increase of the yield stress results in a slower process. In addition nodal pressures are almost constant, as they should be in the applied load case. If fixed velocities are imposed the load happens to be nearly proportional to the viscosity. In such a case the velocities are practically insensitive to variations in the yield stress whereas pressure sensitivity is positive and tends to be linearly proportional to changes in the yield stress for materials exhibiting behaviour close to perfect plasticity.

A similar analysis is performed with the other parameters entering the constitutive model (fluidity $\gamma$, exponent of the viscoplastic law $n$, *cf.* Eq. (1)), and the friction coefficient $f$, *cf.* Eq. (24), as the design parameters. The results for the chosen set of points are shown in Figures 5 to 7, where the velocity, pressure and their design derivatives calculated by direct differentiation (full line) and by FDM (dotted line) are plotted.

It comes out from the sensitivity analysis accounting for the different parameters entering the constitutive model that the fluidity $\gamma$ and the exponent $n$ have negligible effect on the pressure when loads are held constant. It should be noticed that the discrepancies shown in Figure 5d for the pressure sensitivities with respect to the fluidity $\gamma$ are negligible when compared to the pressure. Irregular results are obtained by FDM, which seem to be due to unsufficient precision while solving the perturbed problem and by the truncation errors inherent when the finite length of the perturbation $\delta\gamma$ is taken ($\delta\gamma = 0.01$ in this case). Similarly, irregular sensitivity results for the FDM at the end of the considered interval for $n$ suggest similar errors in the application of this method.

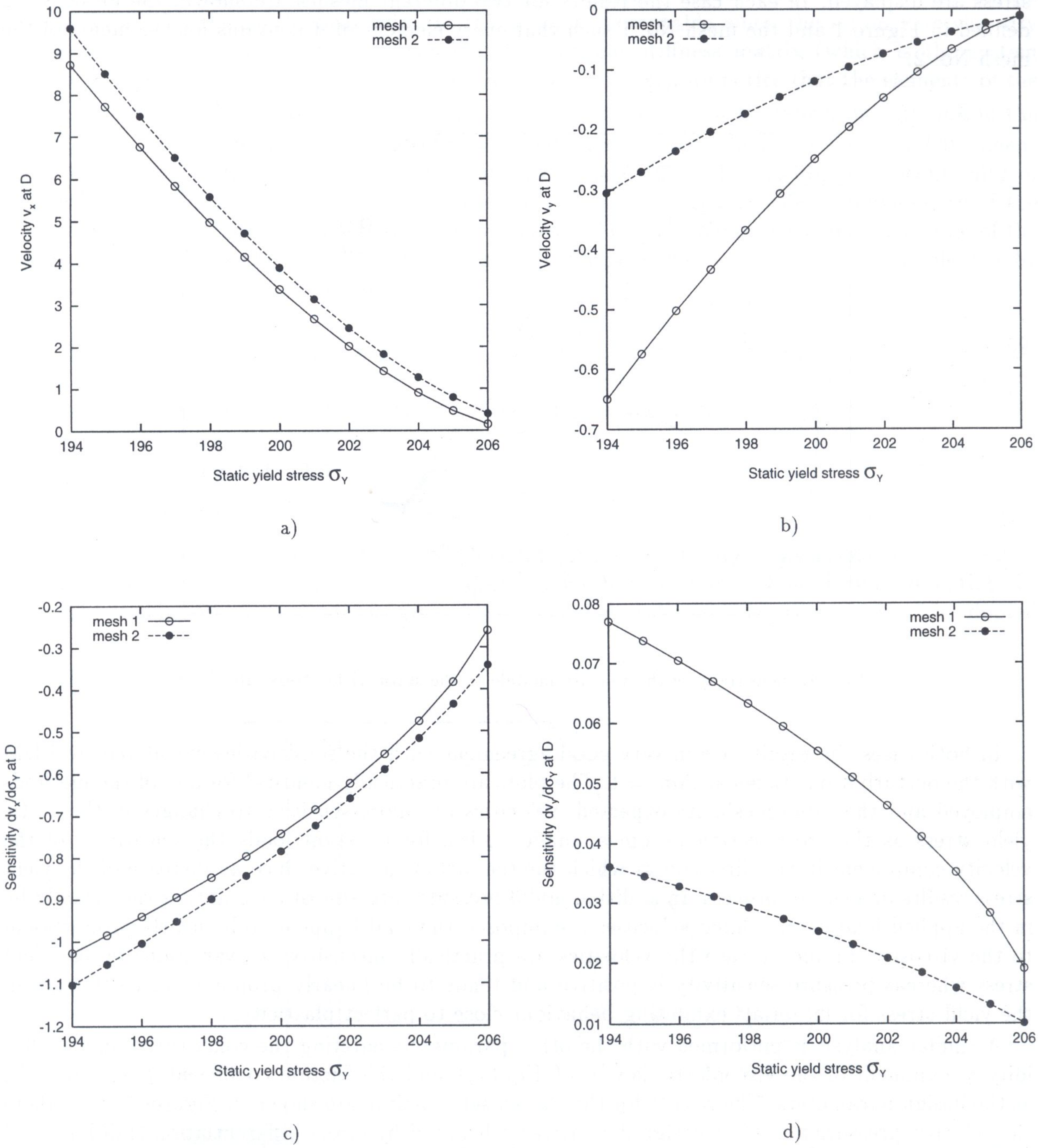


**Fig. 3.** Velocity components and velocity sensitivity coefficients with respect to static yield stress *vs.* static yield stress at point D

Analysis of sensitivity to the friction coefficient $f$ leads to a different situation. Unlike the previous cases analysed, it has been found that the sensitivity coefficients of the problem variables with respect to the friction coefficient calculated by the FDM are very sensitive to the size of the perturbation $\Delta f$ used to calculate the numerical derivatives. In fact, no range of $\Delta f$ was found in which a stable value of sensitivities could be obtained. Considering the friction phenomenon, we can expect a non-smooth transition between the two different friction types: sticking (with zero tangential velocity) and sliding friction. In terms of the friction elements used for this analysis, according to the local pressure value we may find points alternating between both the types of friction along with the changing friction coefficient. The specific friction model we are dealing with

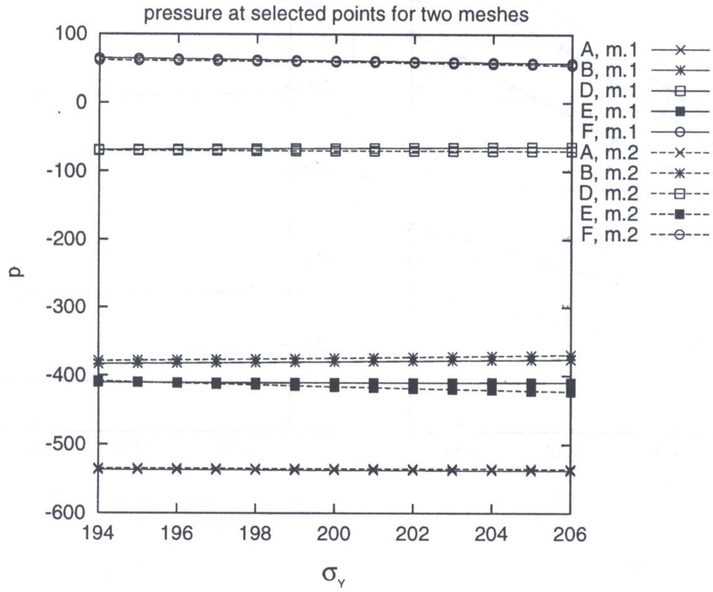


a)

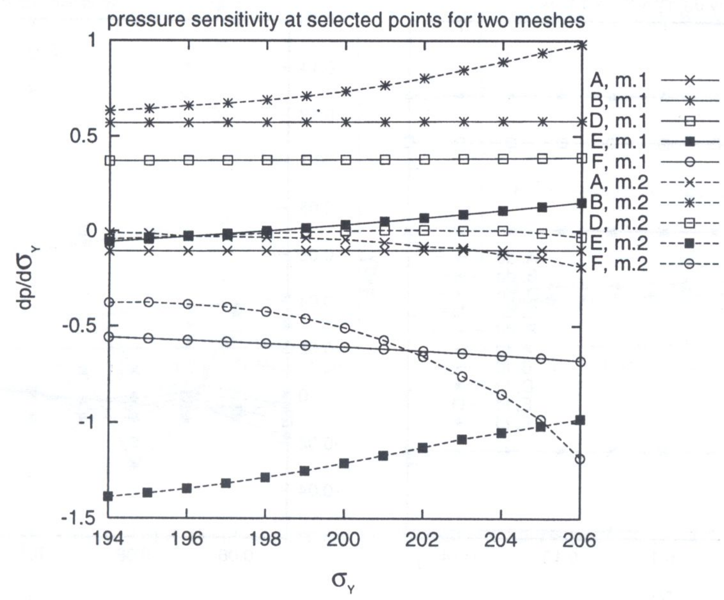


b)

**Fig. 4.** Pressure and pressure sensitivity coefficients with respect to static yield stress *vs.* static yield stress at different points

has two aspects which seem to explain the failure of the sensitivity analysis in this case: the non-smoothness of the friction law, which leads to a discontinuous derivative, and the treatment of the surface phenomenon as a volumetric one, which implies numerical integration over an essentially discontinuous zone. This means that the elements which can give acceptable friction results for

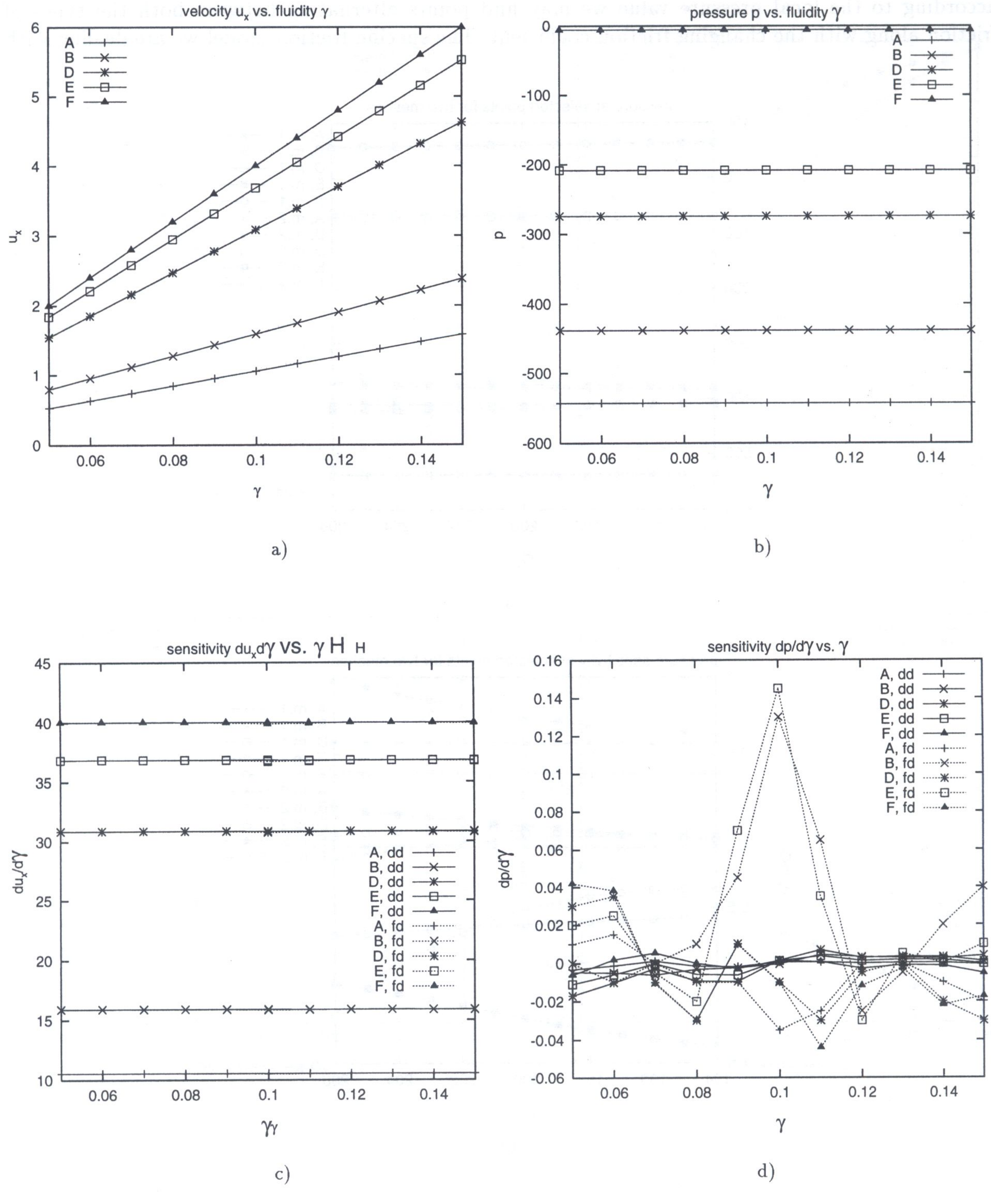


**Fig. 5.** Velocity and pressure, and their sensitivity coefficients with respect to fluidity coefficient *vs.* fluidity coefficient at different points

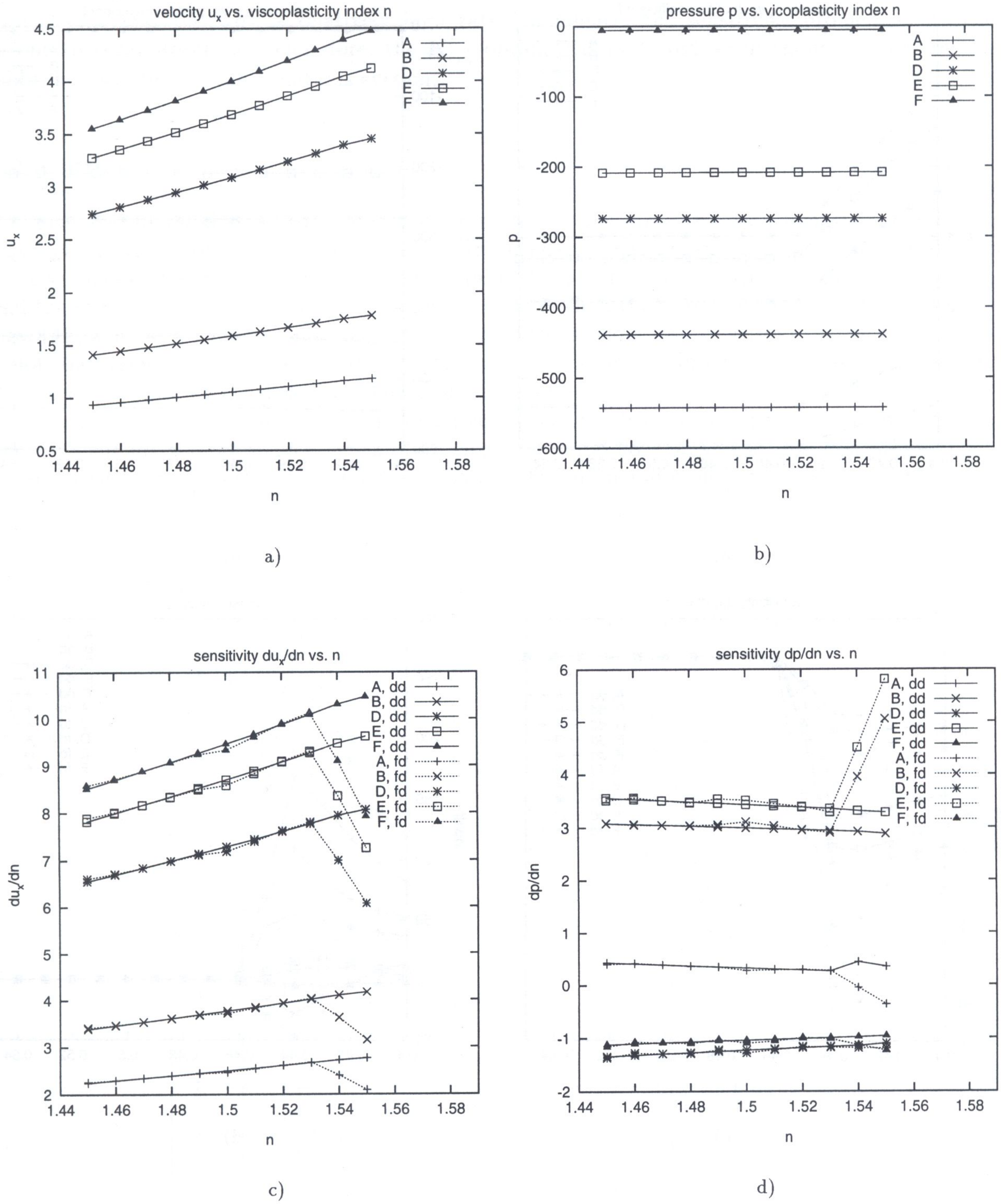


**Fig. 6.** Velocity and pressure, and their sensitivity coefficients with respect to parameter $n$ *vs.* $n$ at different points

the equilibrium problem, are not suitable for sensitivity analysis. We have thus performed the sensitivity analysis by DDM without confronting the results against those of FDM. DDM results are plotted in Figure 7, in which important response changes are obtained until a certain value

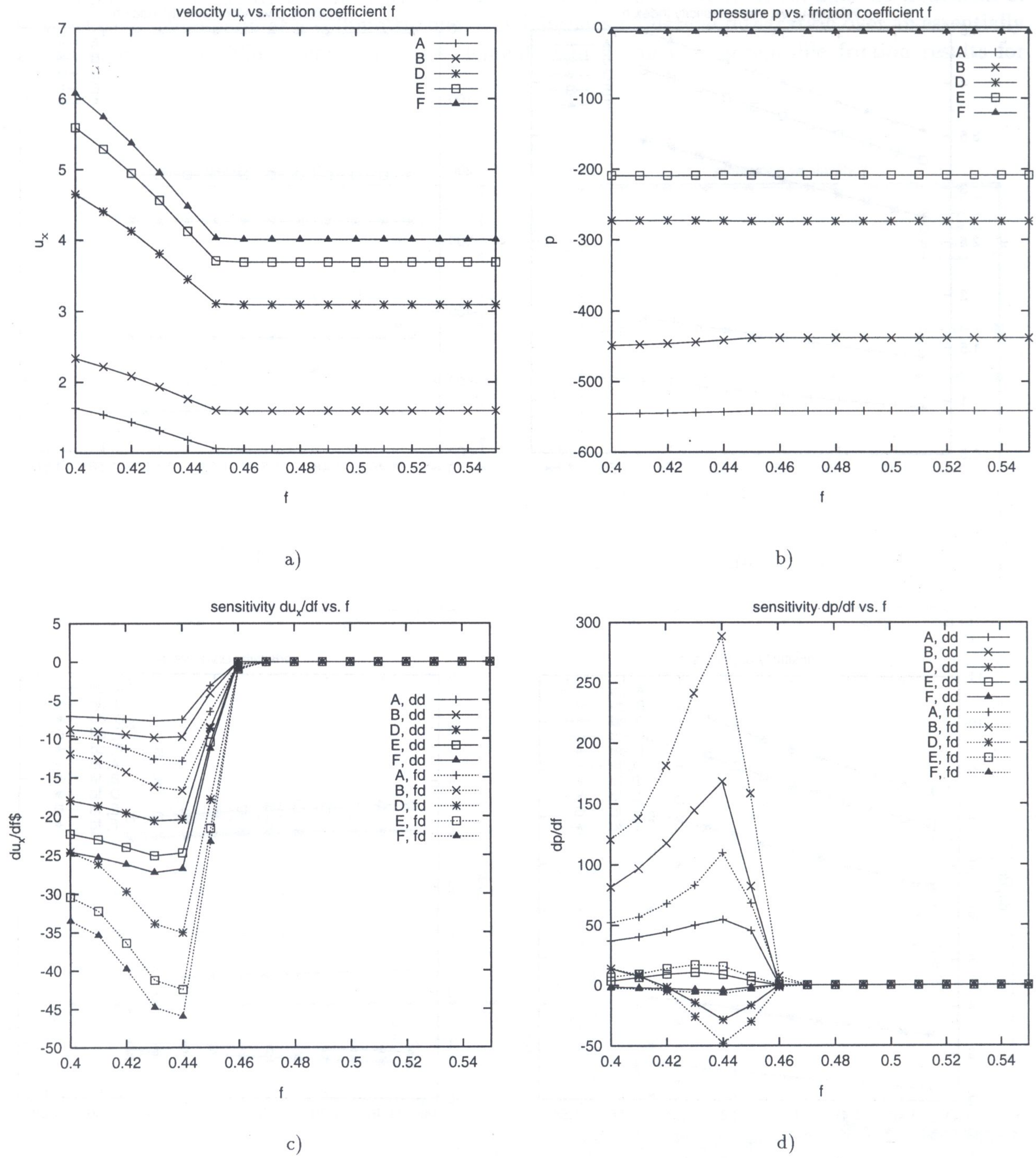


**Fig. 7.** Velocity and pressure, and their sensitivity coefficients with respect to friction coefficient $f$ *vs.* $f$ at different points

of the friction coefficient is reached (for constant value of the imposed extrusion load), starting at which all the boundary exhibits sticking friction and therefore no sensitivity to the friction coefficient appears.

In this example the equilibrium problem has been solved by direct iterations so that the secant stiffness matrix was available at the end of this step. However, since the material properties were typical of a material with a relatively high rate-dependence, the sensitivity problem converged in one to three iterations. Therefore, the $\mathbf{K}^t_{(\mu)}$ option was preferred, even though it required an additional solution of the equations system.

### 5.2. Cutting

We have also found that for low rate-sensitive materials the direct solution method according to Eqs. (34) or (42) is not possible: the tangent matrix is nearly singular, and the numerical inverse does not give the exact solution in one iteration. In spite of that, this matrix, when applied iteratively to find the solution, usually yields convergence much faster than the direct iterative scheme defined by Eqs. (45) and (46). However, in some extreme cases the scheme resulting from the tangent matrix is not convergent, and solution is only possible by direct iterations. In addition, convergence is very slow in such a case and it may take thousands of iterations.

This fact is illustrated in the second example, in which a 2-D cutting problem is simulated by placing a cutting tool at a given depth of an incoming metal flow causing a flow separation: a chip is separated from the main flow. Figure 8a shows the initial finite element mesh used. Constant

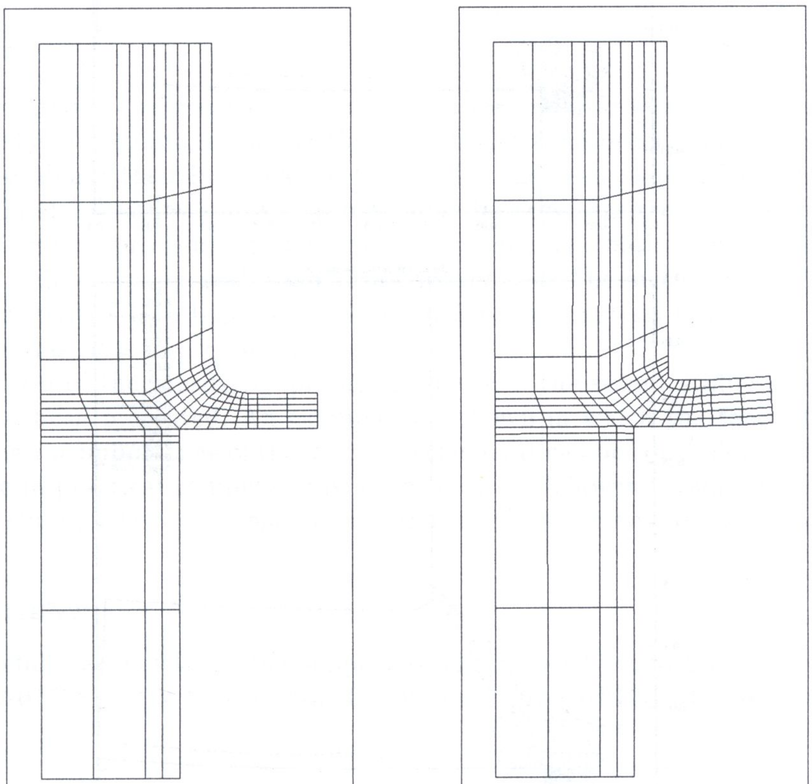

a) b)

**Fig. 8.** Cutting: a) initial mesh, b) final mesh

loads are imposed on the upper boundary of the mesh. The metal properties are those of a nearly perfectly plastic material ($n = 40$ in Eq. (1)). Most of the domain undergoes rigid body flow: almost all the plastic deformation is concentrated in the region where the flow separation takes place. The problem has two free surfaces, which are handled by requiring them to be tangent to the velocity and accordingly updating the nodal coordinates. For the lower surface contact elements impose (via penalty) a restriction to the normal velocity when a no-penetration condition requires so, and release it if normal traction is obtained in the fixed part of the curve. In this way the point where the chip separates from the tool can be determined. Figure 8b shows the final mesh after solution is obtained with fulfillment of the contact and free surface conditions. From the initially smooth

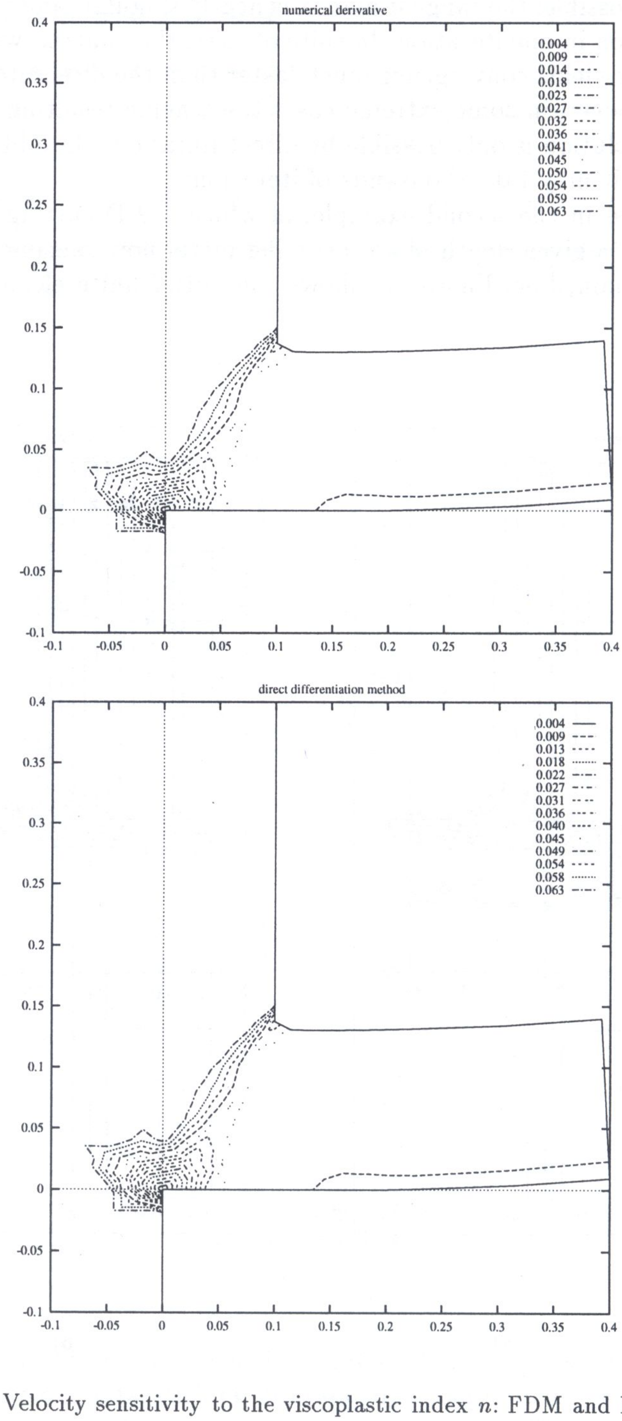


**Fig. 9.** Velocity sensitivity to the viscoplastic index $n$: FDM and DDM

profile assumed at the beginning, a sharp angle is obtained separating two zones of the free surface which correspond to rigid body motion of the respective regions connected by a discontinuity line.

In this example, the iterative scheme given by Eq. (45) had to be applied because of the numerical problems related to the material behaviour mentioned at the beginning of this section. Figure 9 compares the sensitivity of the velocity module to the viscoplastic law index $n$ obtained by the central finite difference approach and the direct differentiation method. Both methods give the same solution which consists, similarly to the velocity field, of subdomains with constant velocity sensitivity separated by a narrow shear deformation rate sensitivity band (i.e. a band with high values of $\mathrm{d}\dot{\varepsilon}_{12}/\mathrm{d}n$) in correspondence with the plastic deformation zone.

The failure in using the tangent matrix (its application leads to divergent results) has a physical interpretation in the fact that a perfectly plastic material is infinitely sensitive to variations in the material properties if constant loads are applied. The whole process is stable if the boundary conditions consist of non-zero imposed velocities; it is then seen that the velocity sensitivities are virtually zero. As a matter of fact, the variations in the applied loads are proportional in this case to the variations of the material parameters; therefore, no response change is observed.

An additional feature arises from this example. We find that changes in a material parameter are reflected in the shape of the problem, since the velocity-pressure field determines the free surfaces (and separation point) location. Therefore there is a coupling between parameter and shape sensitivity analysis. This coupling, however, has not been considered in this paper; it deserves a separate treatment and will be covered in a forecoming paper. For the finite difference verification we considered a fixed domain to calculate the perturbed solutions in order to obtain the corresponding part of the derivative without considering the coupling.

## 6. Conclusions

The parameter sensitivity analysis has been discussed for metal forming problems analysed in the framework of the flow formulation. Taking the constitutive (and other) parameters as design variables the way to evaluate their influence on the results has been shown. The problems modelled with the friction model described in Sec. 2 proved to be very sensitive to changes in the friction coefficient; for this reason problems in finding an optimum perturbation for calculating the derivatives by the finite difference approach have been encountered. The methods proposed in the paper which give the sensitivities as a byproduct of the equilibrium analysis have been demonstrated to work well even for this class of problems, though.

The iterative form of the sensitivity problem, for which the secant stiffness matrix is used for iterations, has also been presented. An example was shown in which the tangent matrix was not applicable implying the importance of the iterative scheme. It can be concluded that such a situation will typically arise in practical computations when both the following conditions hold true: (i) the material model is close to the ideally plastic one, and (ii) there are no prescribed nonzero velocities.

## Acknowledgment

The authors gratefully acknowledge the support of the Polish Committee for Scientific Research (Grant No. 7T07A01508 — the first author, Grant No. 7T07A01810 — the second author).

## References

[1] G. V. Goon, P. I. Poluchin, W. P. Poluchin, B. A. Prudcowsky. *Plastic deformations of metals* (in Russian). Moscow, 1968.

[2] O.C. Zienkiewicz, P.C. Jain, E. Oñate. Flow of solids during forming and extrusion: some aspects of numerical solutions. *Int. J. Solids Structures*, **14**: 15–38, 1978.

[3] O.C. Zienkiewicz, J.S. Campbell. Shape optimisation and sequential linear programming. In: R.H. Gallagher, O.C. Zienkiewicz, eds., *Optimum Structural Design*. Wiley, New York, 1978.

[4] E.J. Haug. A review of distributed parameter structural optimization literature. In: E.J. Haug, J. Cea, eds., *Optimization of distributed parameter structures*. Sijthoff-Nordhoff, Alphen aan den Rijn, 1981.
[5] E.J. Haug, J.S. Arora. *Applied optimal design*. Wiley, New York, 1979.
[6] E.J. Haug, K.K. Choi, V. Komkov. Design sensitivity analysis of structural systems. *Series in Math. Sci. Eng.*, Academic Press, New York, 1986.
[7] Y.S. Ryu, M. Haririan, C.C. Wu, J.S. Arora. Structural design sensitivity analysis of nonlinear response. *Comput. Struct.*, **21**: 245–255, 1985.
[8] R.J. Yang, M.E. Botkin. Accuracy of the domain material derivative approach to shape design sensitivities. *AIAA J.*, **25**: 1606–1610, 1987.
[9] K.K. Raju, G.V. Rao, N. Venugopal. Use of design sensitivity coefficients for prediction of structural behaviour after design modification. *Comput. Struct.*, **33**: 1329–1341, 1989.
[10] M. Kleiber, T.D. Hien, H. Antunez, P. Kowalczyk, Parameter sensitivity of elastoplastic response, *Eng. Comp.*, **12**: 263–280, 1995.
[11] T.J. R. Hughes, L.P. Franca, M. Balestre. A new finite element formulation for computational fluid dynamic: V. Circumventing the Babuska–Brezzi condition: A stable Petrov–Galerkin formulation for the Stokes problems accommodating equal-order interpolations. *Comp. Methods Appl. Mech. Engng.*, **59**: 85–99, 1986.
[12] H.J. Antúnez, S.R. Idelsohn. Topics in numerical solution of isothermal and thermal-coupled forming processes. *Latin Am. Appl. Res.*, **20**: 69–83, 1990.
[13] H.J. Antúnez, *Análisis por elementos finitos del conformado de metales, con orientación a la laminación de tubos sin costura*, Ph.D. dissertation, Universidad Nacional de Córdoba, Argentina, 1990.
[14] A. Karagiannis, H. Mavridis. A finite element convergence study for shear-thinning flow problems. *Int. J. Num. Meth. Fluids*, **8**: 128–138, 1988.